J. E. Purkinje University in Ústí nad Labem
Faculty of Science
Department of Physics

Abstract of doctoral thesis

Metal nano-particles in polymers prepared by ion implantation and their characterization

Petr Malinský

Supervisor: doc. RNDr. Anna Macková, Ph.D.
Consultants: doc. Ing. Vladimír Hnatowicz, DrSc.
RNDr. Martin Švec, Ph.D.

Ústí nad Labem 2015

Univerzita J. E. Purkyně v Ústí nad Labem
Přírodovědecká fakulta
Katedra fyziky

Autoreferát disertační práce

Kovové nanočástice v polymerech připravené iontovou implantací a jejich charakterizace.

Petr Malinský

Školitel: doc. RNDr. Anna Macková, Ph.D.
Konzultanti: doc. Ing. Vladimír Hnatowicz, DrSc.
RNDr. Martin Švec, Ph.D.

Ústí nad Labem 2015

Disertační práce byla vypracována na základě vědeckých výsledků na katedře fyziky Přírodovědecké fakulty Univerzity J. E. Purkyně v Ústí nad Labem a na oddělení neutronové fyziky Ústavu Jaderné Fyziky Akademie Věd ČR, v.v.i. v Řeži v letech 2007–2015 v rámci doktorského studia P1703 Počítačové metody ve vědě a technice.

Doktorand: Mgr. Petr Malinský

Školitel: doc. RNDr. Anna Macková, Ph.D.
Katedra fyziky, PřF, UJEP
České mládeže 8, 400 96 Ústí nad Labem
Oddělení neutronové fyziky, UJF AVČR v.v.i.
Řež 130, 250 68 Řež

Konzultanti: doc. Ing. Vladimír Hnatowicz, DrSc.
Oddělení neutronové fyziky, UJF AVČR v.v.i.
Řež 130, 250 68 Řež

RNDr. Martin Švec, Ph.D.
Katedra fyziky, PřF, UJEP
České mládeže 8, 400 96 Ústí nad Labem

Oponenti: Doc. RNDr. Zdeněk Doležal, Dr.
Ústav částicové a jaderné fyziky, MFF, UK Praha
V Holešovičkách 2, 180 00 Praha 8

Doc. RNDr. Jan Voves, CSc.
Katedra mikroelektroniky, FEL, ČVUT Praha
Technická 2, 166 27 Praha 6

Autoreferát byl odeslán dne .....

Ke stažení je na adrese http://sci.ujep.cz/doktorskestudium-info.html

Obhajoba se koná dne ..... v ..... hodin před komisí pro obhajoby disertačních prací v oboru P1703 Počítačové metody ve vědě a technice na Přírodovědecké fakultě Univerzity J. E. Purkyně v Ústí nad Labem, místnost ....., České mládeže 8, 400 96 Ústí nad Labem. S disertací je možno se seznámit na studijním oddělení Přírodovědecké fakulty Univerzity J. E. Purkyně v Ústí nad Labem.

Předseda OR: prof. RNDr. Rudolf Hrach, DrSc.
Katedra fyziky, PřF, UJEP
České mládeže 8, 400 96 Ústí nad Labem

Abstract

The main topic of the presented work is metal/polymer nano-structures deposition and characterization of their compositional and structural changes, the desired optical and electrical properties, and the morphology of metal nano-particles using different analytical methods. The very important task was the simulation of ion beam interaction with the surfaces with the different morphology. Computer simulations were also employed for the image analysis of the nano-particles. The main aim of this research was to contribute to a better understanding of polymer structure and chemical composition change during the ion implantation with metal ions. Further to the understanding of implanted dopant behaviour in polymers and eventually clustering of metal atoms into the nano-particles and subsequently growth of these nano-particles with increasing ion fluence. And last but not least the change of electrical and optical properties, caused by supplying of the metal portion to a non-conductive pattern and the change of the polymer matrix, was studied.

The work is divided with respect to the used analytical methods, to the used ion implanted specie, to the change of the composition and structure of implanted matrix and eventually changes of the implanted polymer physical properties. Ion beam analytical methods serve for the description of the implanted metal depth profiles in as-implanted and subsequently annealed samples, for the characterization of the compositional changes, especially the hydrogen and oxygen release. The surface morphology have been analysed by Atomic Force Microscopy (AFM). The Transmission Electron Microscopy (TEM) with subsequently computer image analysis has been used to visualize the clustered nano-particles. The measurement of the electrical properties together with the UV-Vis measurement has shown the modification of the physical properties followed in the implanted polymers.

The surface roughness of the analysed samples can influence significantly the interpretation and evaluation of the elemental depth profiles provided by the ion beam techniques. Especially in the case of the implanted and subsequently annealed polymers, when the correct knowledge of the doped depth profiles is needed, the roughness influence should be estimated. Thus we implemented the AFM surface morphology into the back-scattered ion beam spectrum simulation and tested the influence of the surface roughness on the elemental depth profiling provided by Rutherford Back-Scattering analysis (RBS). First step was testing of our developed code on the virtual surfaces, which was generated by computer. The second step was application of the developed code on real samples with the regular roughness.

Keywords: ion implantation, RBS, AFM, simulation of RBS spectra, surface roughness

Abstrakt

Předmětem předkládané disertační práce je příprava nanostruktur kov-polymer a charakterizace jejich kompozitních a strukturálních změn, dále pak studium požadovaných optických a elektrických vlastností a popis morfologie připravených kovových nanočástic s využitím různých analytických metod. Jedním z význačných úkolů byla simulace interakce iontového svazku s povrchy s různou morfologií, počítačové simulace byly také použity pro obrazovou analýzu kovových nanočástic. Hlavním cílem tohoto výzkumu bylo přispět k lepšímu porozumění tomu, jak se mění struktura a chemické složení polymerní matrice během implantace kovovými ionty. Dále pak chování implantovaného dopantu v polymeru, případně klusterování jednotlivých atomů a tvorba nanočástic a jejich následný růst spolu s rostoucí implantovanou dávkou. V neposlední řadě pak byla studována změna elektrických a optických vlastností implantovaných polymerů, způsobená nejen dodáním kovového podílu do nevodivé matrice, ale i změnou této polymerní matrice.

Práce je dělena s ohledem na použité analytické metody, na použitý implantovaný dopant, na změny struktury a složení polymerní matrice a na změny fyzikálních vlastností implantovaných polymerů. Iontové analytické metody poskytly informace o hloubkových profilech implantovaných dopantů v implantovaných i následně žíhaných vzorcích a pomohli charakterizovat změny ve složení polymerní matrice, speciálně pokles vodíku a kyslíku. Povrchová morfologie byla studována metodou mikroskopie atomárních sil (AFM). Transmisní elektronová mikroskopie (TEM) spolu s obrazovou analýzou byly použity k vizualizaci kovových nanočástic. UV-Vis spolu s měřením elektrických vlastností pak definují změny fyzikálních vlastností implantovaných polymerů.

Ukazuje se, že povrchová drsnost analyzovaných vzorků může mít negativní vliv na interpretaci a vyhodnocení hloubkových profilů určených metodou RBS. Speciálně u implantovaných a následně žíhaných vzorků, kdy je třeba relativně přesně určit hloubkový profil dopantu, je vhodné určit tento vliv povrchové drsnosti. Proto jsme v této práci implementovali AFM výsledky popisující povrchovou morfologii do simulace spekter zpětně odražených iontů a následně jsme testovali vliv povrchové drsnosti na hloubkové profily, které poskytuje metoda Rutherfodovy spektroskopie zpětně odražených iontů (RBS). Prvním krokem bylo testování vyvinutého programu na virtuálních površích generovaných počítačem. V druhém kroku jsme se soustředili na reálné vzorky s regulární drsností.

Klíčová slova: iontová implantace, RBS, AFM, simulace spektra RBS, povrchová drsnost

1 Aims of the thesis

The thesis is focused on two main goals, preparation and characterization of nano-composites combing selected metals with common synthetic polymers and methodology of ion based analyses of specimens with imperfect surfaces.

We focused on the following tasks:

i) Preparation of metal-polymer nano-composites using ion implantation and metal deposition;

ii) Characterization of the nano-structured metal/polymer materials using ion beam analytical methods and the additional complementary methods to follow the metal nanoparticle morphology, optical and electrical properties;

iii) Computer simulations of RBS spectra from the samples with different surface roughness and testing and proving of our code by the comparison to the real RBS spectra of the specially designed samples with the regular roughness.

2 Introduction

The composites and nano-composites, consisting from two or more distinct materials, are of high importance for their many special properties. Nano-structured materials, e.g. metal nano-particles embedded in dielectric matrix, have a great application potential due to the specific optical (quantum confinement effect, surface plasmon resonance), electronic (discrete density of states), electrical (single electron transistor), thermal (anomalous specific heat) and magnetic properties (few atom clusters of diamagnetic element showing ferromagnetism) [1–3]. Because of these unique properties, nano-composites may be used to production of optical bandpass filters, optical absorbers and wave-guides, photo-detectors and sensors, energy sources or reservoirs with great power, mechanical components with high strength-to-weight ratio, magneto-sensors and magneto-optical devices which can be used in wide range of human activities.

One of the powerful tools for synthesis of the metal/polymer nano-composites is ion implantation that provides of variety options for selecting parameters of the desired metal particles in a polymer matrix. Ion implantation is an efficient method of modification of solids. At higher ion fluences the implanted atoms aggregate and metal nano-particles are formed. These processes may be well controlled by appropriate choice of metal ions, their energy, current and fluence [4, 5]. A post-implantation annealing temperature and time can further affect growth and size of the metal nano-particles and the resulting optical, magnetic and electrical properties of the implanted samples [4]. A disadvantage of the ion implantation is the fact that the ion irradiation to high fluences (above 10^{15} cm^{-2}) leads to the structural and compositional changes in the irradiated polymer, such as breaking of chemical bonds, escape of volatile fragments, destruction of macromolecules, networking, free radical formation, creation of carbonyl groups, polymer gradual carbonisation and disordering of polymer matrix [4, 6, 7].

Although many works have been published on the metal/polymer nano-composites prepared by ion implantation, there are still many open questions how the nano-particle coalescence depends on the composition/structure of used polymer, on the properties of implanted metal and on the ion implantation parameters. Moreover, the influence of the ion implantation on the structure and chemical composition of polymer matrix is a complex phenomenon, and theory of the chemical and physical interaction between implanted ions and matrix atoms is not completely understood. The problematic is many combinations of ion species and polymer matrix possibility which can be used, and in these all is a wide area for the systematic study of the desired properties after the ion implantation in connection with changes of structural, compositional, optical etc. properties.

Methods of Ion Beam Analysis (IBA), such as Rutherford Backscattering Spectrometry (RBS) or Elastic Recoil Detection Analysis (ERDA), are well established techniques for

quantitative analyses of the near-surface regions of various materials. RBS make it possible to extract the elemental depth profiles with a depth resolution of the order of 10 nm. However, the depth resolution on real samples may adversely be deteriorates by sample-surface roughness and in a worst case precludes the elemental depth profiling in shallow surface layers.

Detailed knowledge of the effects of different types of sample roughness on the RBS spectra is important not only for accurate characterization of real samples but it may give an idea how to get information on the sample structure from the measured RBS spectra. Since the preparation of a set of samples with well-defined roughness is difficult a systematic experimental examination of the roughness effects has not been accomplished up to now. In this situation systematic study of the effects of different types of roughness on RBS spectra simulated in different measuring set-ups by an effective computer simulation seems to be useful.

3 Results and discussion

In the presented study three ferromagnetic metals (Ni, Co and Mn) were used such as implants into the polymer matrix due to their potential electrical and magnetic properties (see Tab. 1). Metal ion implantation supposed to be a good way to prepare the metal precipitates or nano-particles, and behaviour of these metal nano-particles can significantly change the electrical, optical and magnetic properties of implanted polymer matrix/layer.

As the polymer matrix we have chosen the synthetic polymer foils of polyethyleneterephthalate (PET), polyetheretherketone (PEEK) and polyimide (PI) (see Tab. 1), all supplied by Goodfellow, Ltd. These polymers were selected due to being prevalent in industry and high chemical and radiation resistance. Moreover these used polymers differs from the point of view of the glassy transition temperature, ratio of the crystalline and the amorphous phase contained, composition, complexity of monomer unit etc., thus we obtain the systematic study which takes into account all these aspects and simultaneously gives opportunity to compare by the comprehensive way the ion beam modification and nano-particle coalescence taking place in implanted polymers.

Implanted ion specie	Polymer matrix	Implanted ions energy	Ion implantation fluence	Annealing temperature
Nickel	PET, PEEK, PI	40 keV	0.1 – 1.5×10^{17} cm^{-2}	50 – 300 °C
Cobalt	PET, PEEK, PI	40 keV	0.2×10^{16} – 1.0×10^{17} cm^{-2}	200 °C
Manganese	PET, PEEK, PI	80 keV	0.1 – 1.0×10^{16} cm^{-2}	200 °C

Table 1: Experimental conditions of ion beam implantation

Metal depth profiles in polymers

The depth profiles of three transition metals (Ni, Co and Mn) implanted into different polymers (PET, PEEK and PI) were measured by using RBS and compared with those simulated with SRIM and TRIDYN codes. SRIM code includes Monte Carlo (MC) full cascade and is able to provide the reasonable ion implanted depth profiles in materials that are radiation stable and more less stable under the ion beam. TRIDYN has implemented the compositional and volume density changes as is changed during the implantation process.

It is evident, that the concentration maximum of implanted metals move to the sample surface for fluences up to 1.0×10^{16} cm^{-2} (see Fig. 1 left). The shift with the increasing ion fluence is also reproduced in the TRIDYN simulation. The shape of the implanted depth profiles shows a Gaussian distribution for ion fluences below 7.5×10^{16} cm^{-2} and change dramatically from the fluence of 1.0×10^{17} cm^{-2} and higher with the concentration maximum moving on the sample surface. These changes of the concentration depth profiles and

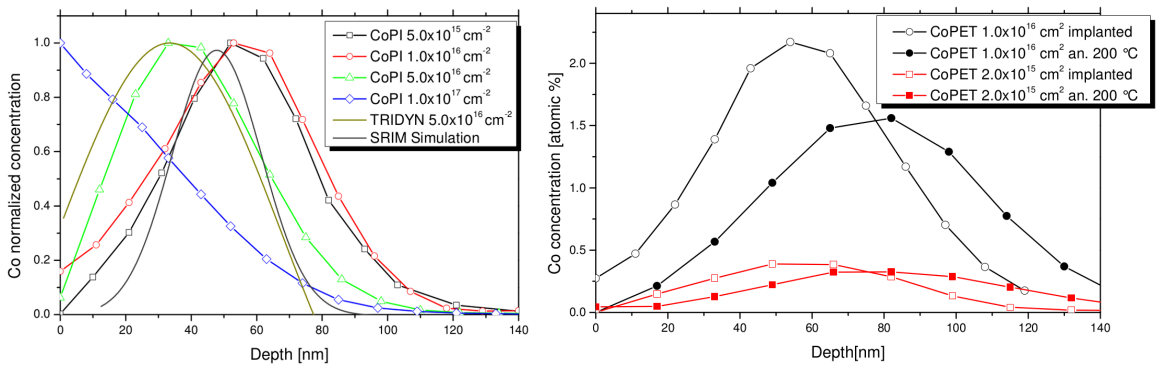

Figure 1: **Left** The Co depth profiles in the PI implanted at the different fluences compared with the SRIM and TRIDYN simulation (TRIDYN simulation is performed with the fluence of 5.0×10^{16} cm^2) [12]. **Right** The concentration depth profiles of the Co atoms in PET before and after the annealing at 200 °C for 20 min [13].

profile shift to the sample surface are caused by progressive polymer degradation, sputtering and gradual compositional and structural changes of polymer matrix [4,8,9].

After annealing of implanted polymer samples a measurable shift to greater depths of profile concentration maxima is observed (see Fig. 1 right). The shift is most pronounced in PET. The shift of the depth profiles after the annealing can be caused by the thermally stimulated diffusion of the metal atoms or particles. The annealing of the polymers implanted to higher fluences, in which the concentration of the implanted atoms exceeds their solubility, leads to the migration and aggregation of the implanted atoms [9].

The measured depth profiles of all implanted metals differ from those simulated by SRIM for the samples implanted to fluences above 1.0×10^{16} cm^{-2} (Fig. 1 left). The disagreement between measured and predicted implanted profile parameters at high implantation fluences (above 1.0×10^{16} cm^{-2}) is not surprising since the SRIM code does not take into account progressive structural and compositional changes in the polymer matrix caused by ion irradiation. The structural changes during ion irradiation can be better described with the help of the TRIDYN code (see Fig. 1 left), where the dynamic changes in sample thickness and composition during the implantation are taken into the account (sputtered atoms, density enhancement via the impurity atom implantation). However, nor TRIDYN results are not in accord with our experimental data for the ion fluences above 1.0×10^{17} cm^{-2}. The discrepancy is due to some effects which are not included into TRIDYN simulation (e.g. inward movement of a part of implanted atoms from the site of implantation, faster surface sputtering and atom diffusion) [9].

Compositional changes in polymers under ion implantation

Polymer degradation during the ion implantation is accompanied by release of volatile or gaseous degradation products enriched by hydrogen and/or oxygen. This well-known process leads to a gradual carbonization of the ion-irradiated surface layer of polymers [9, 14–

16]. The carbonization causes matrix compaction and the increase of its density. Analysis of the light elements desorption in polymer matrix and depth profiling of these elements was accomplished by the RBS and ERDA methods.

The metal ion implantation to fluences above 1.0×10^{17} cm^{-2} leads to the complete dehydrogenation of PET and PEEK surface (see Fig.2 left). The surface of PI foil was completely dehydrogenated only in the case of the Ni implantation. The highest decrease in hydrogen concentration was observed in PET in all experiments with different ion species and ion energies used. The irradiation of PET, with the simplest monomer (only one aromatic ring), to high fluences leads to the bond breaking, destruction of the ester group and release of volatile fragments [9]. The hydrogen release observed from PI was lowest, which is in agreement with the fact, that this polymer has three aromatic groups in monomer and has highest endurance against the ionizing radiation. Another important factor is the fraction of nuclear energy loss which become prevailing at low ion energies and is mostly responsible for massive polymer destruction [4]. The thickness of the hydrogen depleted layer for the ion fluences up to 1.0×10^{16} cm^{-2} correlates well with the maximal range of the implanted ions and for higher fluences the thickness of dehydrogenated layer enlarges. The additional enlargement of the dehydrogenated layer can be connected with the compositional and density change of the surface layer during ion implantation and subsequent increase of the collision cascades length due this change.

For all polymers the Mn^+ irradiation leads to greater oxygen depletion comparing to the Ni^+ and Co^+ irradiation (see Fig. 2 right), what effect may be connected with the great difference between the Gibbs free energy of Ni and Co oxides comparing to Mn oxides [1]. It may be concluded, that the hydrogen release is more significant in comparison with the oxygen one. The difference can be due to differences in desorption processes. The resulting

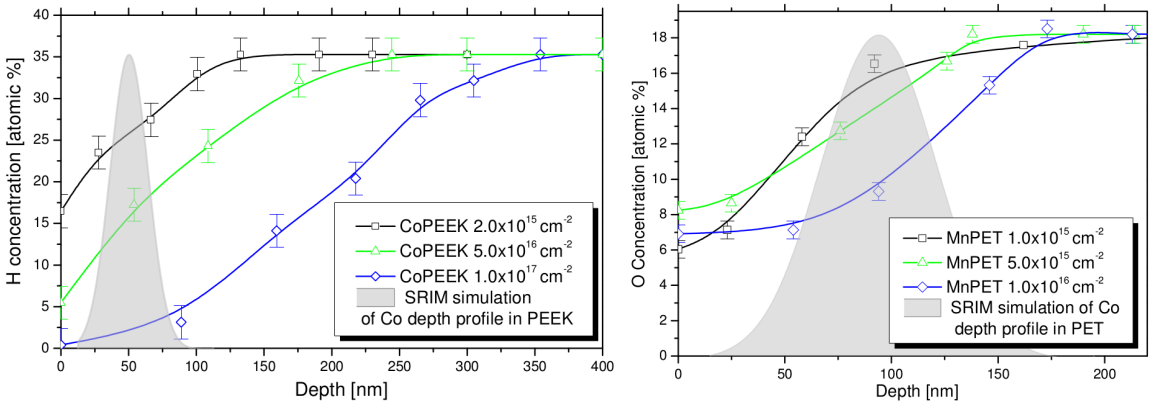

Figure 2: **Left** Hydrogen concentration depth profiles determined from ERDA spectra of PEEK implanted with 40 keV Co^+ ions to different fluences [12]. **Right** The oxygen concentration depth profiles spectra of PET implanted with 80 keV Mn^+ ions to different fluences [18]. The SRIM calculated 40 keV Co and 80 keV Mn depth profile in PET is attached.

oxygen concentration may be affected by adsorption of oxygen from the ambient atmosphere during implantation process and storage of the samples on the air when oxygen is bound on the dangling bonds produced by ion bombardment [4,14]. The adsorption may significantly affect the oxygen concentration depth profile too.

Subsequent annealing of implanted samples can lead to both decrease or increase of the oxygen content in the modified layer depending on the polymer type, implanted specie properties and structural changes induced by ion irradiation [8]. The polymers implanted to high fluences exhibit a significant carbon enrichment in structures with conjugated bonds in the implanted layer. The carbonized surface layer represents a diffusion barrier for oxygen migrating from the ambient atmosphere as was shown in [4]. In the case of Co^+ implantation, the annealed PET and PI exhibit further oxygen depletion, but in PEEK slight oxygen enrichment in the ion implanted layer is found. On the other side, in the case of Mn the subsequent oxygen enrichment in the annealed PET and PEEK is observed, in contrast with PI, where the oxygen concentration depth profile does not change after annealing in comparison with the as-implanted sample. This can be connected with the fact, that the used Mn implantation fluences were below the threshold of complete polymer carbonization (see also [4]).

Surface morphology of ion implanted polymers

It is well known that the ion implantation leads to changes in the surface morphology of implanted polymers which are related to compositional changes, desorption of the sample mass and possibly to other processes. On the other hand the altered surface morphology (increased surface roughness) may affect the physico–chemical properties of the specimens and last but not least the result of RBS or ERDA analyses. In this part we will present the AFM analysis and change in the PET, PI and PEEK surface morphology after irradiation with Ni^+, Co^+ and Mn^+ ions.

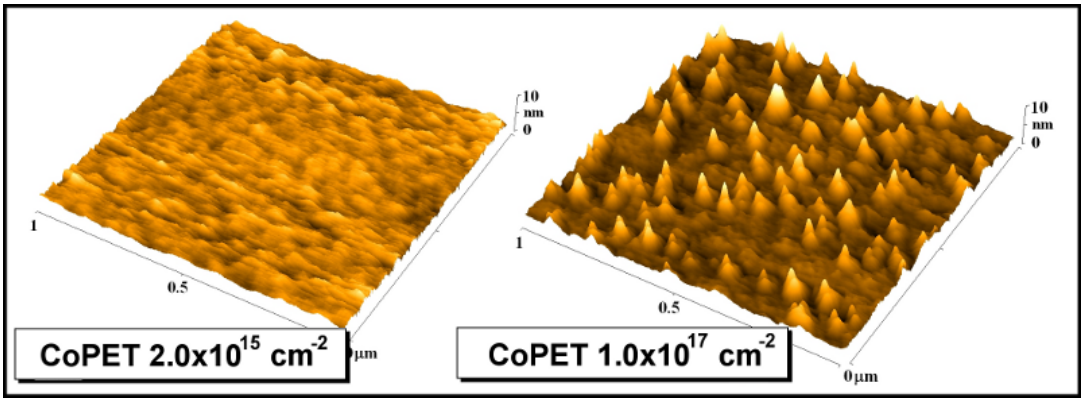

Figure 3: The AFM surface morphology of PET implanted by Co^+ ions at fluences of 2.0×10^{15} cm^{-2} and 1.0×10^{17} cm^{-2} [12].

It may be concluded that the ion irradiation of polymers leads, in general, to an increase of polymer surface roughness, the increase depending on the polymers chemical structure. The effect is observed for all used metal ions, especially for Ni^+ implantation. The most pronounced changes in the surface morphology and the surface roughness increase was observed on the PEEK for all three used implanted metals. The PEEK has relative complex monomer and the higher fraction of crystalline phase. On the other hand, in the case of PI, with the pronounced fraction of amorphous phase and with the most complex monomer [19], a surface smoothing has been observed after implantation to ion fluences up to 1.5×10^{17} cm^{-2}. The "spiky" structure appears on the PET and PEEK surface implanted to the highest fluences (see Fig. 3). This effect can be associated with the different structure of the pristine polymers and processes of chain scission or polymer chain packing during the implantation [20].

In general the annealing up to temperature of 200 °C results in a slight increase of surface roughness (characterized by R_a and RMS parameters) for all used polymers and metals. The largest increase is observed in the case of PET for all three implanted metals. The effect may be related to lower glass transition temperature T_g of PET and the crystallization increasing with increasing temperature above of T_g [21].

Results of XPS and UV-VIS analysis

The results of UV–Vis and XPS were used for the characterization of the degradation process in irradiated polymers and for characterization of polymeric chains and metal particles clustering. UV-Vis spectrometry results may be interpreted either as fingerprints of optically absorbing clusters, or as hints for the production of benzene-, quinone-, or fullerene-enriched matters [9]. The analysis of the XPS spectra allows the binding energies and chemical states description near the surface of implanted polymers.

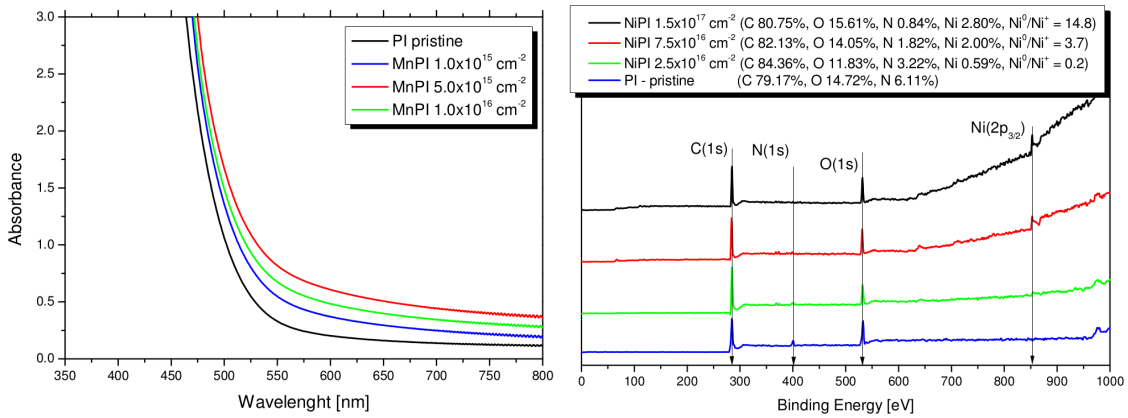

Figure 4: **Left** Typical UV–Vis spectra of the PI implanted with Mn^+ ions to different fluences [18]. **Right** Typical XPS spectra of the Ni^+ implanted PI. The ratio of Ni^0/Ni^+ is attached [10].

The UV-Vis absorbance increases dramatically for the PET and PEEK after the implantation with all metals starting from the lowest ion fluence. With increasing ion fluence the UV-Vis absorbance gradually continues to growth. On the other side, in the PI samples implanted by Ni^+, Co^+ and Mn^+ ions the UV-Vis absorbance increases gradually already for the lowest fluences (see Fig. 4 left). This optical properties change corresponds to the compositional changes during ion implantation. The absorption enhancement with increasing ion fluence indicates a growth of conjugated double bonds concentration in the polymer chain as well as charge carrier concentration [23, 24]. It may be concluded that metal implantation creates compact carbonaceous clusters which are responsible for a narrower optical band gap and higher optical absorbance [25, 26]. The largest number of carbon atoms in cluster together with the lowest value of the optical band gap is observed in PI with more complex monomer unit compared to PET and PEEK (see Tab. 2).

Polymer	Ion fluence [cm^{-2}]	E_g [eV]	N
PEEK	Pristine	3.11	~ 122
	5.0×10^{15}	3.07	~ 125
	1.0×10^{17}	3.00	~ 131
PI	Pristine	2.22	~ 239
	5.0×10^{15}	2.05	~ 280
	1.0×10^{17}	1.91	~ 322

Table 2: The variation of indirect band gap E_g, number of carbon atoms N as a result of irradiation at different Co fluences [12].

The XPS was used especially for the polymers irradiated to extremely high ion fluences, where the metal nano-particles coalescence and the significant changes of chemical structure is expected. It was proven that the metal presence becomes XPS observable only for the ion fluences above 7.5×10^{16} cm^{-2} (see Fig. 4 right). In the case of lower fluences (up to 1.0×10^{16} cm^{-2}) no metal fraction is observed.

TEM and Image Analysis

Implanted Ni, Co and Mn atoms may diffuse and agglomerate spontaneously into metal nano-particles of different size. This clustering of metal atoms depends on the used implant and his fluence and on the used polymer matrix. In this thesis the TEM imaging and subsequent image analysis was used for the displaying of created nano-particles and to determine their size distribution.

The nano-particles agglomeration was proved in PET, PEEK and PI implanted with all metals to fluences above 2.5×10^{16} cm^{-2} for Ni^+ (see Figs. 5 and 6) and above 1.0×10^{16} cm^{-2} for Co^+ and Mn^+. On the other hand, for the ion implantation to ion fluences below 1.0×10^{16} cm^{-2} the creation of metallic nano-particles cannot be visualized as they are too small. The

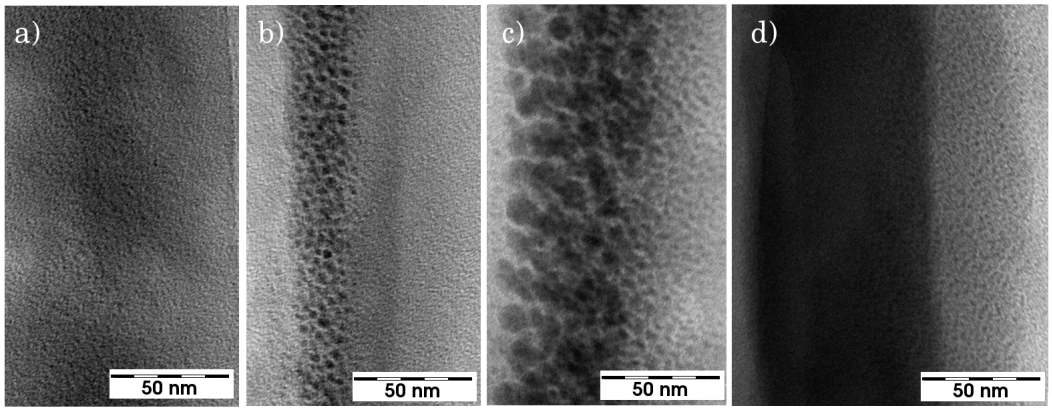

Figure 5: The TEM images of PET implanted with 40 keV Ni^+ ions to the fluences of a) 2.5×10^{16} cm^{-2}, b) 5.0×10^{16} cm^{-2}, c) 7.5×10^{16} cm^{-2} and d) 1.5×10^{17} cm^{-2} [11].

fastest rate of the nano-particles growth was observed in PET, regardless of implanted metal, which has the lowest viscosity of polymer matrix. It was found that the morphology of the newly formed metal nano-phase is to a great extent controlled by the viscosity of the polymer matrix [27]. The subsequent annealing of PET implanted with Ni results in a decrease of the nano-particle size comparing to the as-implanted samples. In the case of Ni^+ implanted PI and PEEK no significant change in nano-particle size was observed after the annealing.

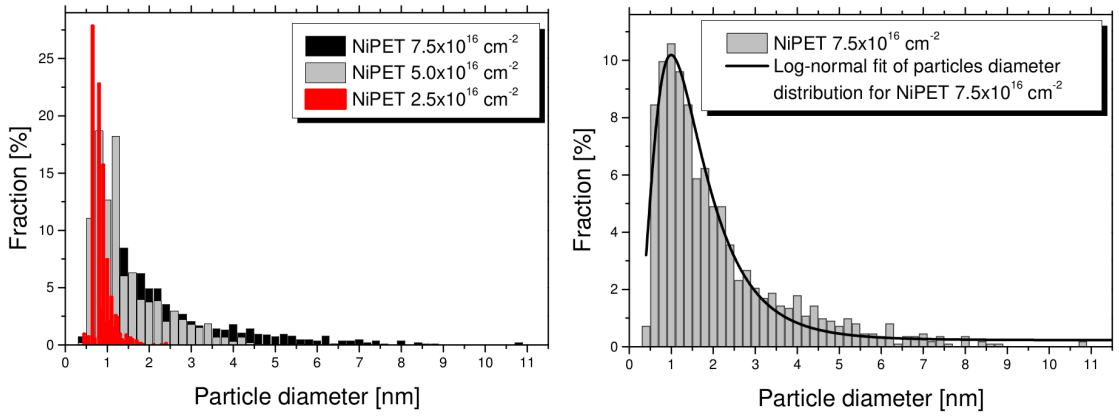

Figure 6: The Ni particle distribution determined from TEM images of PET implanted with 40 keV Ni^+ ions to the different fluences (left) and the log-normal fit of particle diameter distribution for PET implanted to the fluence of 7.5×10^{16} cm^{-2} (right).

Electrical properties of prepared nano-structures

The polymers ion implantation to high fluences using of metal implants leads to several phenomena that may change significantly the electrical properties of the implanted polymer. The metal concentration increasing, nano-particles agglomeration and polymer compositional change due the ion irradiation, which leads to the carbonization of surface layer

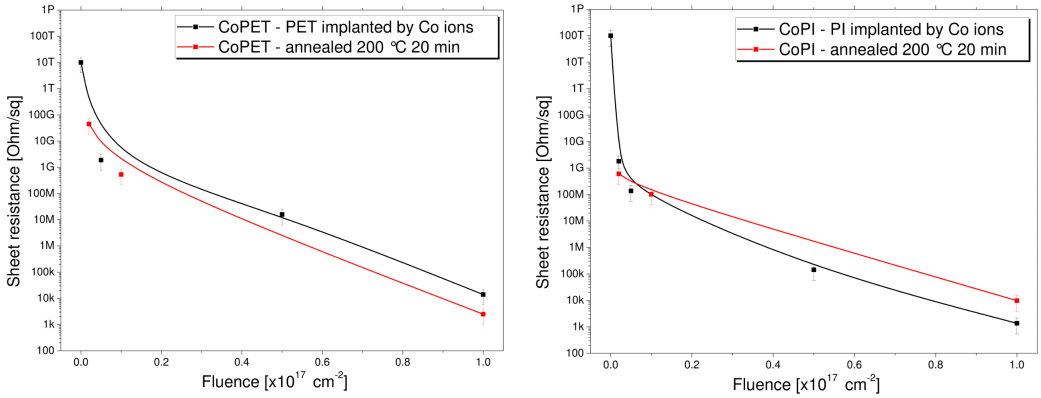

Figure 7: The electric resistance of Co^+ as-implanted and annealed PET and PI [13].

are some of the most important change that influences the conductivity/resistivity of the implanted sample.

The sheet resistance of the ion implanted polymers is a decreasing function of the ion fluence (see Fig. 7). The decrease is caused by the growing concentration of conjugated double bonds and the production of carbonaceous clusters, which, at higher ion fluences, may form systems of conductive paths [4, 8]. The conductivity of the implanted layer is strongly dependent on the peculiarities of the morphology of the carbonaceous phase (the size of carbon clusters, character of their linking in aggregates and on the presence of heteroatoms) [27]. After the annealing the no significant changes of the sheet resistance was observed in the investigated polymers in the frame of uncertainties of the used measuring two point method.

Computer simulation of surface roughness influence on the of RBS analysis

Two simple codes were written for simulation of rough surface influence on the RBS spectra. The first code was written in Delphi-Pascal and is designed for the simulation of backscattered ion spectra on the hypothetical virtual structures, the name of this code is *DP-Rough*. The virtual structures of rough surface are generated as the part of *DP-Rough* simulation. The second code was written in FORTRAN 95 and can be used for the simulation of RBS spectra on real rough samples with using of the data obtained from AFM. The name of this code is *F95-Rough*. The basic concept of the present codes is to generate large number of particular RBS spectra for ions impinging the sample surface at different, randomly chosen positions and scattered under identical conditions (Fig. 8). The final RBS spectrum is obtained as a sum of the particular RBS spectra. To take into account the fine features of the sample surface properly, large number of ion trajectories has to be generated.

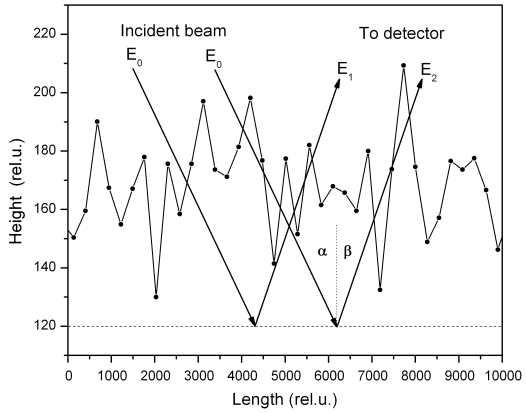

Figure 8: Schematic theoretical implementation of the surface roughness into RBS spectra generation considering the used geometry. Primary beam with energy E_0 comes under the incident angle α and scattered beam leaves the sample under the exit angle β, both measured with respect to the substrate surface normal. Two typical trajectories are shown (heavy lines) for ions scattered at the same depth.

Simulation of RBS spectra from virtual rough surface

The effects of different types of surface roughness on RBS spectra is demonstrated by *DP-Rough* simulation on the samples comprising either rough layer deposited on smooth substrate or smooth layer deposited on rough substrate. From large variety of possible simulation results some typical examples were shown. The simulation is highly simplified and several minor processes affecting ion passage through matter are omitted in order to speed up the calculation. The code enables to generate samples with different types of surface or interface roughness and to calculate, in tolerable time, large number of particular RBS spectra from ion trajectories, randomly distributed over the sample.

Significant deformation of the RBS signal from the rough layer is observed for grazing incident and exit angles (see Fig. 9 right). The effect of roughness periodicity was illustrated on the virtual generated layer with triangular roughness with constant and randomly distributed thickness (see Fig. 9 left). The effect of periodicity on the RBS spectrum is well visible from the shape of the simulated RBS spectrum in the low energetic part of the layer signal. The *DP-Rough* generated RBS spectra from the virtual samples comprising smooth layer on rough substrate are sensitive not only to substrate relief but also to measuring geometry.

Simulation and measurement of RBS spectra on real samples

The *F95-Rough* code uses 2D cuts of the sample surface obtained by the AFM method as input information (see Fig. 10). The feasibility of the code is demonstrated on RBS spectra of samples with well defined regular surface morphology and on RBS spectra of the polymer samples implanted by Co^+ ions. The samples with regular surface morphology were

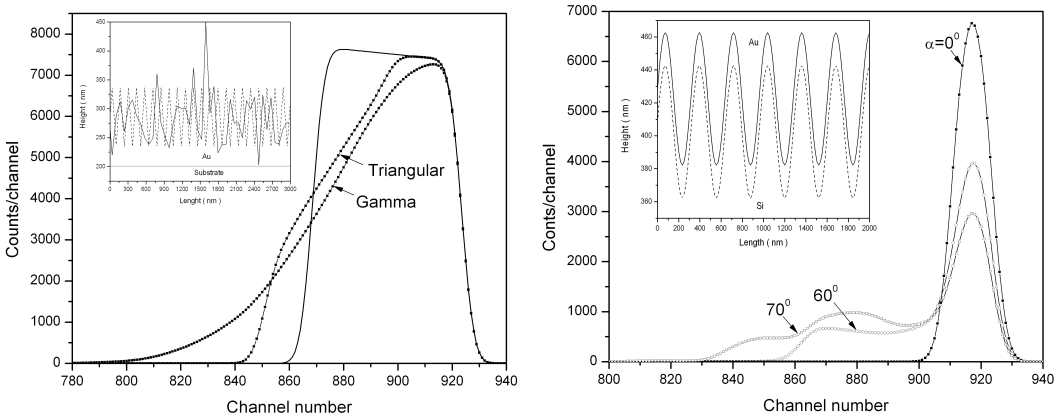

Figure 9: **(Left)** Comparison of RBS spectra from the Au layer with saw–like profiles–periodic with constant amplitude ± 50 nm (Triangular) and amplitudes generated from Gamma distribution with $\sigma/d_m = 0.6$ (Gamma). In both cases the mean layer thickness was $d_m = 85$ nm. **(Right)** Relevant part of simulated RBS spectra from the sample comprising thin Au layer ($d_m = 20$ nm) deposited on Si substrate with periodic sinusoidal relief, measured in standard geometry ($\alpha = 0°$, $\beta = 15°$) and under two glancing angles $\alpha = 60°$ and $70°$. The laboratory scattering angle was always $165°$.

prepared by the sputtering of a 35-nm-thick gold layer on the surface of the PET substrate periodically patterned by laser irradiation.

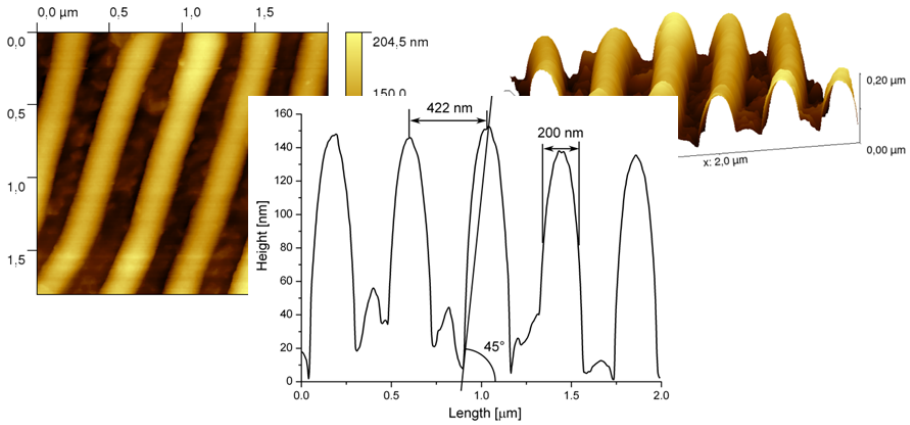

Figure 10: AFM images of the Au/PET pattern prepared by laser beam with incoming angles of 45°. The 2D AFM images are shown on the left, the 3D morphology is depicted in the left and the extracted 2D cut (cross-section) profiles, used for the spectra simulations, are shown at the bottom.

It becomes obvious that the *F95-Rough* code reproduces the main features of the measured RBS spectra at least qualitatively (see Fig. 11 left). The discrepancies between the measured and simulated spectra are mostly attributable to the uncertainty in the surface-morphology obtained by AFM, the possible inhomogeneity of the sputtered gold layer and the limited accuracy of the simulation. It should be noted that in general the appearance of the multi-peak gold signal in the RBS spectra reflects surface periodic structure. The *F95-Rough* simulation shown, that the surface roughness of polymers implanted by metal

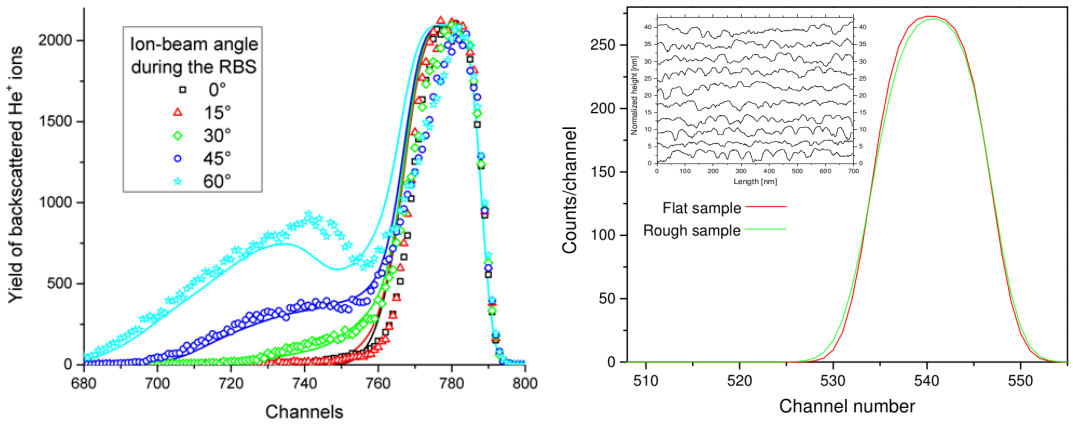

Figure 11: **Left** Experimental RBS spectra (points) of samples with regular roughness measured at different ion beam-incidence angles, are compared with those simulated (lines) by our code using real 2D AFM surface profile. The spectra were obtained from the samples prepared by laser irradiation under the angle 0°. **Right** Part of simulated RBS spectra of 2 MeV He^+ ions, corresponding to Co signal, scattered from the rough and flat PI sample comprising Co layer. The 2D cuts of PI surface are shown inset.

ions (see Fig. 11 right) has not significant influence on the concentration depth profiles of implanted specie in this case. It was expected, that roughness parameters much less than the depth resolution of the analytical methods can't influence significantly the elemental depth profile, but this is not usual case, thus such analysis is very important for the further investigation of micro- and nano-structures prepared by ion beam writing and ion beam micro-machining.

Conclusion

The presented Thesis is focused on the very frequently problematic study of nowadays - the fundamental physical properties of metal/polymer nano-composites and the novel analytical methods for their characterization. The metal/polymer nano-composites in our case were deposited using ion implantation and their properties were studied using the wide portfolio of the analytical techniques (RBS, ERDA, AFM, TEM, UV-Vis, XPS, sheet resistance measurement). The structural and compositional change of the implanted polymers matrix and physical properties induced by ion implantation were studied in terms of the polymer type and ion implanted species.

A significant hydrogen and oxygen release, associated to the monomer complexity and prevailing nuclear stopping power, from the polymer surface after the ion implantation was detected simultaneously with surface carbonisation and growth of the carbon clusters. The carbon atoms have tendency to create clusters with sp^2 electronic state hybridization. This type of chemical bonding between carbons possesses unpaired π-electrons which become charge carriers in the implanted polymers [4]. The increase of the charge carrier density in polymer matrix is accompanied by decrease of the sheet resistance and the optical band gap. Except the conductive carbon-rich layer formation, the metal nano-particle growth is expected as the process that contributes to the change of the optical and electrical properties of implanted polymers. TEM shows us the morphology of the grown metal nano-particles and was concluded, that the polymer viscosity and metal chemical activity influenced the nano-particle grow. From XPS analysis can be deduced, that the nano-particles starting the growth as the metal-oxides compounds and the metallic state increases with increasing ion fluence. The ion implantation of polymers causes the significant increase of the surface roughness that is connected to the interaction of low energy ions with polymer structure and subsequent large sputtering effect and chain scission. In general RBS evaluation of the shallow elemental depth profiles suffers by the surface roughness increasing, thus the novel software was developed to the simulation of RBS spectra with the implementation of surface morphology. This code enables to get information about the elemental depth distribution from rough samples and potentially can be used for the extraction of the roughness parameters from RBS spectra. Simulation of the surface roughness influence of implanted polymers on the metal depth profiles determined by RBS was performed.

In summary, we have obtained a large set of the original experimental data on metal-polymer nano-structures, concerning the many aspects of their fundamental physical properties, which were published in respectable impacted journals, simultaneously our data were used and cited by many scientists which are interested in this research field e.g. in reviews [4, 8]. Simultaneously we presented novel simulation approach for the surface roughness implementation into the RBS spectra generation, which is irreplaceable especially in case of very shallow elemental depth profiles evaluation, where the surface roughness can play crucial role.

Závěr

Předkládaná disertace se soustředí na často citovanou problematiku současnosti a to na základní fyzikální vlastnosti nano-kompozitu kov/polymer a na analytické metody pro popis těchto vlastností. Nano-kompozity kov/polymer byly v našem případě připravovány metodou iontové implantace a jejich vlastnosti byly studovány řadou moderních analytických metod (RBS, ERDA, AFM, TEM, UV-Vis, XPS, měření plošného odporu). Změny ve struktuře a složení implantovaných polymerů byly studovány s ohledem na typ polymeru a kovového implantantu.

Po iontové implantaci byl v modifikovaných vzorcích detekován výrazný úbytek kyslíku a vodíku, který je ovlivněn komplexitou monomeru a poměrem elektronových a jaderných brzdných ztrát implantovaných iontů. S degradací polymeru po iontové implantaci je spojena karbonizace povrchu modifikovaného vzorku a růst uhlíkových klatrů. Uhlík má tendenci k tvorbě klastrů s sp^2 elektronovými slupkami, které jsou hybridizovány. Tento typ chemických vazeb mezi uhlíky obsahuje nespárované π-elektrony, ze kterých se stávají nosiče náboje v implantované vrstvě [4]. Nárust množství volných nosičů náboje je doprovázen poklesem plošného odporu a optického zakázaného pásu modifikovaných polymerů. Dalším procesem, který přispívá ke změně elektrických a optických vlastností je vznik a růst kovových nanočástic. TEM byla použita k popisu morfologie rostoucích nanočástic a s naměřených výsledků lze předpokládat, že růst kovových nanočástic je ovlivněn viskozitou polymeru a chemickou aktivitou implantovaného kovu. Z výsledků metody XPS může být vyvozováno, že nanočástice vznikají jako sloučeniny kov-oxid a spolu s rostoucí implantovanou dávkou přechází do kovového stavu. Po iontové implantaci dochází u modifikovaných polymerů k nárustu povrchové drsnosti, která má přímou souvislost s interakcí nízko energetických kovových iontů se strukturou polymeru a následným odprašováním povrchu polymeru a rozrušováním polymerních řetězců. Obecně, nárust povrchové drsnosti může ovlivnit hloubkové profilování metodou RBS. Proto byl v rámci disertace vyvinut jednoduchý program, který umožňuje implementovat povrchovou drsnost analyzovaného vzorku do simulace spektra RBS. Následně byl tímto programem testován vliv drsnosti analyzovaných vzorků na měřené hloubkové profily implantovaných kovů.

V rámci disertace jsme obdrželi velké množství experimentálních dat, popisujících fyzikální vlastnosti nano-struktur kov/polymer, které byly publikovány v respektovaných impaktovaných časopisech. Zároveň byla část získaných dat použita a citována v publikacích týkající se podobné problematiky, např. v přehledech [4, 8]. Jako součást disertace byla prezentována simulační procedura, která umožňuje implementovat povrchovou drsnost analyzovaných vzorků do spekter RBS.

References

[1] A. L. Stepanov, R. I. Khaibullin, *Optics of metal nanoparticles fabricated in organic matrix by ion implantation*, Rev. Adv. Mater. Sci. 7 (2004) 108–125

[2] S. Dhara, *Formation, Dynamics, and Characterization of Nanostructures by Ion Beam Irradiation*, Crc. Rev. Sol. State 32 (2007) 1–50

[3] G. Cao, Y. Wang, *Nanostructures and nanomaterials - Synthesis, properties, and applications*, World Scientific Publishing Co., Singapore (2011), ISBN 978-981-4322-50-8

[4] V.N. Popok, *Ion implantation of polymers: formation of nanoparticulate materials*, Rev. Adv. Mater. Sci. 30 (2012) 1–26

[5] C. Okay, B.Z. Rameev, R.I. Khaibullin, M. Okutan, F. Yildiz, V.N. Popok, B. Aktas, *Ferromagnetic resonance study of iron implanted PET foils*, Phys. Stat. Sol. 203 (2006) 1525–1532

[6] T. Sasuga, H. Kudoh, *Ion irradiation effects on thermal and mechanical properties of poly(ether–ether–ketone)(PEEK)*, Polymer 41 (2000) 185–194

[7] R. Endrst,V. Svorcik, V. Rybka, V. Hnatowicz, *Surface modification of polymers induced by ion implantation*, Radiat. Eff. Defects S. 137 (1995) 25–28

[8] V.N. Popok, R.I. Khaibullin, A. Toth, V. Beshliu, V. Hnatowicz, A. Mackova, *Compositional alteration of polyimide under high fluence implantation by Co^+ and Fe^+ ions*, Surf. Sci. 532–535 (2003) 1034–1039

[9] Fink D.:*Fundamentals of Ion-irradiated Polymers*, Springer, Berlin, Heidelberg (2004), ISBN 978-3-662-07326-1

[10] A. Mackova, J. Bocan, R.I. Khaibullin, V.F. Valeev, P. Slepicka, P. Sajdl, V. Svorcik, *Characterisation of Ni implanted PEEK, PET and PI*, Nucl. Instrum. Meth. B 267 (2009) 1549–1552

[11] P. Malinsky, A. Mackova, V. Hnatowicz, R.I. Khaibullin, V.F. Valeev, P. Slepicka, V. Svorcik, M. Slouf, V. Perina, *Properties of polyimide, polyetheretherketone and polyethyleneterephthalate implanted by Ni ions to high fluences*, Nucl. Instrum. Meth. B 272 (2012) 396–399

[12] A. Mackova, P. Malinsky, R. Miksova, R.I. Khaibullin, V.F. Valeev, V. Svorcik, P. Slepicka, M. Slouf, *The characterization of PEEK, PET and PI implanted with Co ions to high fluences*, Appl. Surf. Sci. 275 (2013) 311–315

[13] A. Mackova, P. Malinsky, R. Miksova, H. Pupikova, R.I. Khaibullin, V.F. Valeev, V. Svorcik, P. Slepicka, *Annealing of PEEK, PET and PI implanted with Co ions at high fluencies*, Nucl. Instrum. Meth. B 307 (2013) 598–602

[14] E.H. Lee, M.B. Lewis, P.J. Blau, L.J. Mansur, *Improved surface-properties of polymer materials by multiple ion-beam treatment*, J. Mater. Res. 6 (1991) 610–628.

[15] P. Slepicka, S. Trostova, N.S. Kasalkova, Z. Kolska, P. Malinsky, A. Mackova, L. Bacakova, V. Svorcik, *Nanostructuring of polymethylpentene by plasma and heat treatment for improved biocompatibility*, Polym. Degrad. Stabil. 97 (2012) 1075–1082

[16] P. Slepicka, S. Trostova, N. S. Kasalkova, Z. Kolska, P. Sajdl, V. Svorcik, *Surface Modification of Biopolymers by Argon Plasma and Thermal Treatment*, Plasma Process. Polym. 9 (2012) 197–206

[17] J.F. Ziegler, J.P. Biersack, M.D. Ziegler, *SRIM – The stopping and range of ions in matter*, SRIM Co., Chester (Maryland) (2008), ISBN: 096542071X

[18] A. Mackova, P. Malinsky, R. Miksova, H. Pupikova, R.I. Khaibullin, P. Slepicka, A. Gombitová, L. Kovacik, V. Svorcik, J. Matousek, *Characterization of PEEK, PET and PI implanted with Mn ions and sub-sequently annealed*, Nucl. Instrum. Meth. B 325 (2014) 89–96

[19] V. Svorcik, E. Arenholz, V. Hnatowicz, V. Rybka, R. Öchsner, H. Ryssel, *AFM surface investigation of polyethylene modified by ion bombardment*, Nucl. Instrum. Meth. B 142 (1998) 349–354

[20] W. Keith Fisher, J.C. Corelli, *Effect of ionizing radiation on the chemical composition, crystalline content and structure, and flow properties of polytetrafluoroethylene*, J. Polym. Sci. Part A 19 (1981) 2465–2493.

[21] G. Groeninckx, *Viscoelasticity, ultimate mechanical properties and yielding mechanisms of thermally crystallized polyethylene terephthalate*, in Polymer Processing and Properties ed. G. Astarita and L. Nicolais, Springer Science and Business Media, New York (1984), ISBN: 978-1-4612-9716-1

[22] G. Zhou, R. Wang, T.H. Zhang, *Analysis of surface morphological change in PET films induced by tungsten ion implantation*, Nucl. Instrum. Meth. B 268 (2010) 2698 - 2701

[23] D. Fink, R. Klett, L.T. Chadderton, J. Cardoso, R. Montiel, H. Vazquez, A.A. Karanovich, *Carbonaceous clusters in irradiated polymers as revealed by small angle X-ray scattering and ESR*, Nucl. Instrum. Meth. B 111 (1996) 303–314

[24] S. Gupta, D. Choudhary, S. Sharma, *Study of carbonaceous clusters in irradiated polycarbonate with UV–vis spectroscopy*, J. Polym. Sci. B 38 (2000) 1589–1594

[25] G.D. Cody, T. Tiedje, B. Abeles, B. Brooks, Y. Goldstein, *Disorder and the Optical-Absorption Edge of Hydrogenated Amorphous Silicon*, Phys. Rev. Lett. 47 (1981) 1480–1483

[26] J. Tauc, R. Grigorovici, A. Vancu, *Optical Properties and Electronic Structure of Amorphous Germanium*, Phys. Stat. Sol. 15 (1996) 627-637

[27] D. V. Sviridov, *Chemical aspects of implantation of high-energy ions into polymeric materials*, Russ. Chem. Rev. 71 (2002) 315–327

[28] F. Schiettekatte, *Fast Monte Carlo for ion beam analysis simulations*, Nucl. Instrum. Meth. B 266 (2008) 1880–1885

[29] P. Pusa, T. Algren, E. Rauhala,*Fast Monte Carlo simulation for elastic ion backscattering*, Nucl. Instrum. Meth. B 219–220 (2004) 95–98

[30] M. Mayer, *SIMNRA, a Simulation Program for the Analysis of NRA, RBS and ERDA*, AIP Conf. Proc. 475 (1999) 541

Author's articles in impacted journals (the author's participation)

[1] P. Slepicka, P. Jurík, P. Malinsky, A. Macková, N. Slepicková Kasálková, V. Švorcík, *Biopolymer nanostructures induced by plasma irradiation and metal sputtering*, Nucl. Instrum. Meth. B 332 (2014) 7—10 (12%)

[2] A. Mackova, P. Malinsky, H. Pupikova, P. Nekvindova, J.Cajzl, Z. Sofer, R. A. Wilhelm, A. Kolitsch, J. Oswald, *The structural changes and optical properties of $LiNbO_3$ after Er implantation using high ion fluencies*, Nucl. Instrum. Meth. B 332 (2014) 74—79 (30%)

[3] A. Mackova, P. Malinsky, Z. Sofer, M. Mikulics, R. A. Wilhelm, *A study of the structural and magnetic properties of ZnO implanted by Gd ions*, Nucl. Instrum. Meth. B 332 (2014) 80—84 (20%)

[4] A. Mackova, P. Malinsky, R. Miksova, V. Hnatowicz, R.I. Khaibullin, P. Slepicka, V. Svorcik, *Characterisation of PEEK, PET and PI implanted with 80 keV Fe^+ ions to high fluencies*, Nucl. Instrum. Meth. B 331 (2014) 176—181 (40%)

[5] A. Mackova, P. Malinsky, H. Pupikova, P. Nekvindova, J.Cajzl, B. Svecova, J. Oswald, R. A. Wilhelm, A. Kolitsch, *A comparison of the structural changes and optical properties of $LiNbO_3$, Al_2O_3 and ZnO after Er^+ ion implantation*, Nucl. Instrum. Meth. B 331 (2014) 182—186 (20%)

[6] R. Mikšová, A. Macková, P. Malinsky, V. Hnatowicz, P. Slepicka, *The stopping powers and energy straggling of heavy ions in polymer foils*, Nucl. Instrum. Meth. B 331 (2014) 42—47 (10%)

[7] A. Mackova, P. Malinsky, R. Miksova, H. Pupikova, R.I. Khaibullin, P. Slepicka, A. Gombitová, L. Kovacik, V. Svorcik, J. Matousek, *Characterization of PEEK, PET and PI implanted with Mn ions and sub-sequently annealed*, Nucl. Instrum. Meth. B 325 (2014) 89—96 (40%)

[8] P. Souček, T. Schmidtová, V, Buršíková, P. Vašina, Y. T. Pei, J. Th. M. De Hosson, O. Caha, V. Peřina, R. Mikšová, P. Malinský, *Tribological properties of nc-TiC/a-C:H coatings prepared by magnetron sputtering at low and high ion bombardment of the growing film*, Surf. Coat. Tech. 241 (2014) 64–73 (10%)

[9] P. Nekvindova, J.Cajzl, B.Svecova, A. Mackova, P.Malinsky, J.Oswald, J.Vacík, J.Špirkova, *Erbium diffusion from erbium metal or erbium oxide layers deposited on the surface of various $LiNbO_3$ cuts*, Optic. Mat. 36 (2013) 402–407 (20%)

[10] A. Mackova, P. Malinsky, Z. Sofer, P. Simek, D. Sedmidubsky, M. Mikulics, R. A. Wilhelm, *A study of the structural properties of GaN implanted by various rare-earth ions*, Nucl. Instrum. Meth. B 307 (2013) 446–451 (20%)

[11] A. Mackova, P. Malinsky, R. Miksova, H. Pupikova, R. I. Khaibullin, V. Svorcik, P. Slepicka, *Annealing of PEEK, PET and PI implanted with Co ions at high fluencies*, Nucl. Instrum. Meth. B 307 (2013) 598—602 (40%)

[12] A. Mackova, P. Malinsky, R. Miksova, R. I. Khaibullin, V. F. Valeev, V. Svorcik, P. Slepicka, M. Slouf, *The characterization of PEEK, PET and PI implanted with Co ions to high fluences*, Appl. Surf. Sci. 275 (2012) 311—315 (40%)

[13] A. Schaub, P. Slepicka, I. Kasparkova, P. Malinsky, A. Mackova, V. Svorcik, *Gold nanolayer and nanocluster coatings induced by heat treatment and evaporation technique*, Nanoscale Res. Lett. 8 (2013) 249 (15%)

[14] J. Cajzl, P. Nekvindova, B. Svecova, A. Mackova, P. Malinsky, J. Oswald, J. Vacik, J. Spirkova, *Electric field-assisted erbium doping of $LiNbO_3$ from melt*, Scripta Mater. 68 (2013) 739—742 (20%)

[15] P. Slepicka, P. Jurik, Z. Kolska, P. Malinsky, A. Mackova, I. Michaljanicova, V. Svorcik, *A novel method for biopolymer surface nanostructuring by platinum deposition and subsequent thermal annealing*, Nanoscale Res. Lett. 8 (2012) 671 (12%)

[16] P. Malinsky, P. Slepicka, V. Hnatowicz, V. Svorcik, *Early stages of growth of gold layers sputter deposited on glass and silicon substrates*, Nanoscale Res. Lett. 7 (2012) 241 (30%)

[17] P. Slepicka, S. Trostova, N. Slepickova Kasalkova, Z. Kolska, P. Malinsky, A. Mackova, L. Bacakova, V. Svorcik, *Nanostructuring of polymethylpentene by plasma and heat treatment for improved biocompatibility*, Polym. Deg. Stab. 97 (2012) 1075—1082 (10%)

[18] P. Nekvindova, B.Svecova, J.Cajzl, A. Mackova, P.Malinsky, J.Vacík, J.Oswald, A. Kolitsch, J.Špirkova, *Erbium ion implantation into different crystallographic cuts of lithium niobate*, Optic. Mat. 34 (2012) 652–659 (20%)

[19] P. Malinsky, A. Mackova, V. Hnatowicz, R.I. Khaibullin, V.F. Valeev, P. Slepicka, V. Svorcik, M. Slouf, V. Perina,*Properties of polyimide, polyetheretherketone and polyethyleneterephthalate implanted by Ni ions to high fluences*, Nucl. Instrum. Meth. B 272 (2012) 396–399 (40%)

[20] P. Malinský, A. Macková, P. Nekvindová, B. Švecová, M. Kormunda, A. Kolitsch, *Characterization of silicate glasses implanted with Ag^+ ions*, AIP Conf. Proc. 1412, 327 (2011); doi: 10.1063/1.3665331 (18%)

[21] M. Kormunda, J. Pavlik, A. Mackova, P. Malinsky, *Characterization of off-axis single target RF magnetron, co-sputtered iron doped tin oxide films*, Surf. Coat. Tech. 205 (2010) S120–S124 (15%)

[22] B. Svecova, P. Nekvindova, A. Mackova, P. Malinsky, A. Kolitsch, V. Machovic, S. Stara, M. Mika, J. Spirkova, *Study of Cu^+, Ag^+ and Au^+ ion implantation into silicate glasses*, J. Non-Cryst. Sol. 356 (2010) 2468–2472 (10%)

[23] A. Mackova, P. Malinsky, B. Svecova, P. Nekvindova, R. Grotzschel, *Study of Er^+ ion-implanted lithium niobate structure after an annealing procedure by RBS and RBS/channelling*, Nucl. Instrum. Meth. B 268 (2010) 2042–2045 (20%)

[24] P. Slepicka, A. Vasina, Z. Kolska, T. Luxbacher, P. Malinsky, A. Mackova, V. Svorcik, *Argon plasma irradiation of polypropylene*, Nucl. Instrum. Meth. B 268 (2010) 2111–2114 (12%)

[25] P. Malinsky, A. Mackova, J. Bocan, B. Svecova, P. Nekvindova, *Au implantation into various types of silicate glasses*, Nucl. Instrum. Meth. B 267 (2009) 1575–1578 (20%)

[26] A. Mackova, P. Malinsky, J. Bocan, V. Svorcik, J. Pavlik, Z. Stryhal, P. Sajdl, *Study of Ag and PE interface after plasma treatment*, Phys. Stat. Sol. C 5 (2008) 964–967 (15%)

[27] A. Mackova, V. Svorcik, P. Sajdl, Z. Stryhal, J. Pavlik, P. Malinsky, M. Slouf, *RBS, XPS, and TEM study of metal and polymer interface modified by plasma treatment*, Vacuum 82 (2007) 307–310 (10%)

[28] A. Mackova, V. Svorcik, V. Hnatowicz, P. Malinsky, J. Bocan, R. I. Khaibullin, P. Nekvindova, *Material analyses and modification on the tandetron accelerator*, AIP Conf. Proc. 958 (2007) 56–59 (10%)